A Double-Quantum Solid-State NMR Technique for Determining Torsion Angles in Polymers

K. Schmidt-Rohr

Department of Polymer Science & Engineering and Materials Research Science & Engineering Center, University of Massachusetts, Amherst, Massachusetts 01003

Received November 17, 1995; Revised Manuscript Received March 20, 1996[⊗]

ABSTRACT: This paper introduces a double-quantum solid-state NMR experiment for determining torsion angles in unoriented polymers which contain segments with pairs of ^{13}C-labeled sites separated by only one or two bonds. By double-quantum excitation and evolution, two-dimensional spectra are obtained in which the first dimension displays the sum of the anisotropic chemical shifts. As a consequence, the two-dimensional spectral patterns depend on the relative orientation of the coupled sites and thus on the torsion angle. The double-quantum approach achieves homonuclear dipolar decoupling in the first dimension without multiple-pulse sequences and removes the natural-abundance background signal. The experiment is demonstrated on polyethylene isotopically labeled with dilute (∼4%) ^{13}C−^{13}C spin pairs and confirms the all-trans structure in the crystalline regions. In polypeptides, it will be applicable to the determination of the backbone torsion angle ψ in a doubly ^{13}C-labeled amino acid residue, with a sensitivity to analyze one residue in a repeat unit comprising up to 20 residues.

Introduction

The experimental elucidation of molecular conformations in unoriented solids, such as amorphous polymers, unoriented polypeptides, or polycrystalline proteins, is a great challenge. For instance, stringent experimental tests of rotational-isomeric-state models for amorphous polymers, in terms of the backbone torsion-angle distribution itself, are still lacking. Solid-state nuclear magnetic resonance (NMR) provides a set of techniques that show great potential for determining molecular conformations on the level of individual bonds, by probing relative segmental orientations[1−10] or internuclear distances[11−16] through various anisotropic nuclear interactions, such as dipolar couplings and chemical shifts.

Particularly detailed information on torsion angles and their distributions can be obtained by correlating NMR interaction-tensor orientations in two-dimensional (2D) NMR spectra without magic-angle spinning (a related approach based on rotational resonance[7] will be discussed below). The techniques are based on 2D exchange NMR[1−6,17] or on correlation of dipolar couplings with the chemical shifts,[8−10] mostly on specifically ^{13}C labeled samples. However, no torsion angles around backbone carbon−carbon bonds have been determined, even though such data would be valuable for many synthetic and biological polymers. The basis of such a chemical-shift correlation approach, the direct relation between the torsion angle ψ and the relative orientation of chemical-shift tensor principal-axes systems which is amenable to 2D NMR, is visualized in Figure 1, for polyethylene (a) and for a glycine residue in a peptide (b).

The lack of 2D exchange spectra for samples with directly bonded ^{13}C-spin pairs is mostly due to problems with the exchange NMR technique when applied to such ^{13}C−^{13}C systems. Due to the small internuclear distance between the ^{13}C nuclei, the homonuclear dipolar coupling is strong and produces nearly inextricable spectral patterns. The 2D exchange experiment would then require efficient simultaneous ^{13}C−^{13}C and ^{13}C−^{1}H decoupling in both spectral dimensions, which is difficult to implement. In addition, the 2D exchange spectra are dominated by an intense diagonal ridge, which does not provide conformational information. Another NMR technique considered for such systems, two-dimensional correlation of a one-bond ^{13}C−^{13}C dipolar coupling and the chemical-shift anisotropy, provides information on the torsion angle only in a special case, namely, in the intermediate coupling regime[9] (otherwise, the spectra depend only on the orientation of the ^{13}C−^{13}C vector in the chemical-shift principal-axes systems). Therefore, the advantages of directly bonded ^{13}C-labeled segments, such as the relative simplicity of isotopic labeling of adjacent sites and the dependence of the spectra on a single torsion angle, have not been exploited so far.

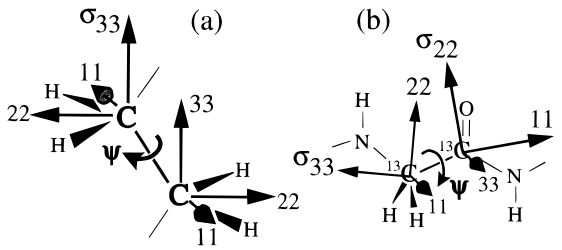

Figure 1. Schematic representation of chemical-shift tensor orientations and the relevant torsion angle ψ for ^{13}C−^{13}C spin pairs in (a) polyethylene and (b) a glycine residue in a peptide. For simplicity, the trans conformations are shown ($\psi = 180°$). The torsion angle determines the relative orientation of the segment-fixed chemical-shift tensors, which can be probed by two-dimensional NMR experiments.

In this paper, we describe a novel double-quantum solid-state NMR technique that achieves useful NMR tensor correlation in ^{13}C−^{13}C labeled segments. It yields two-dimensional spectra with a first spectral dimension, ω_1, that reflects the torsion angle in terms of the sum of the chemical shifts of the coupled sites, without any interference from the dipolar coupling, regardless of the coupling strength. The conformational information is enhanced by correlation with the individual chemical shifts and the dipolar coupling in the directly detected ω_2 dimension. Favorable features of this double-quantum experiment are the inherent removal of the natural-abundance background signal,

[⊗] Abstract published in *Advance ACS Abstracts,* May 1, 1996.

S0024-9297(95)01710-4 CCC: $12.00

which may dominate the spectrum in complex systems, and the absence of the intense diagonal ridge that dominates exchange spectra. We demonstrate the double-quantum technique on polyethylene with dilute (~4%) $^{13}C-^{13}C$ spin pairs. The potential of this approach for distinguishing segmental conformations is illustrated by spectral simulations for doubly ^{13}C-labeled polypeptides.

Experimental Section

The experiments were performed on a Bruker MSL 300 NMR spectrometer at a ^{13}C resonance frequency of 75 MHz. The sample was inserted into the 7 mm coil of a double-resonance Bruker magic-angle-spinning probehead and measured without spinning. 90° pulse lengths were 4.3 μs. The proton decoupling field strength during evolution and detection was approximately $\gamma B_1/(2\pi) = 80$ kHz. A cross-polarization[18] time of 500 μs and a signal-acquisition time of 7 ms were used.

In all the spectra, the signal from the mobile amorphous regions of polyethylene was suppressed on the basis of their short T_1 relaxation time. The suppression is achieved by a "T_1 filter", where the magnetization generated by cross polarization is immediately rotated to the $+z$ and $-z$ axes in alternating scans. During the ensuing 1-s delay, the magnetization of the amorphous phase relaxes to the $+z$ direction. Flipping the crystalline-phase magnetization back to its original transverse direction results in the cancellation of the amorphous-phase signal in every other scan. After the T_1 filter, the actual pulse sequence is started.

For the 2D experiments, the resonance frequency was set such that the spectrum in the ω_1 dimension was off-resonance. In the t_1 dimension, 64 slices with increments of 28 μs were acquired. To obtain a flat double-quantum excitation profile across a range of dipolar-coupling strengths from 3200 to 300 Hz, spectra with eight values of the double-quantum excitation and reconversion delays, 2τ = 140, 280, ..., 1120 μs, were averaged directly during signal acquisition. The measuring time for the full, highly resolved spectrum with very good signal-to-noise ratio was 18 h, or a total of 16 000 scans. To demonstrate the sensitivity of the technique, a 1-h, 1024-scan 2D spectrum with slightly reduced resolution (32 t_1 increments and a single 2τ = 120 μs) is also shown below. The spectral simulations were performed with an angular resolution of 1° on a Power Macintosh 7100/66, requiring less than 30 s/spectrum even in a full calculation without A_2 or AX approximations for the spin system.

The doubly labeled polyethylene was prepared by Ziegler–Natta polymerization of a mixture of 5% doubly ^{13}C-labeled ethene with 95% unlabeled ethene gas. From the ratio of the spin-pair to the natural-abundance signal, the fraction of spins in labeled pairs was determined as approximately 4%.

NMR Theory

Dipolar Couplings and the Double-Quantum Pulse Sequence. Before discussing double-quantum spectroscopy, it is appropriate to review spectral complications in spin-pair systems with strong homonuclear couplings.[9,19,20] They arise from the noncommutation of the homonuclear dipolar or J coupling and the chemical-shift difference Hamiltonians. If the strengths D of the dipolar coupling and Δ of the chemical-shift difference are similar, $D \sim \Delta$, the line positions and intensities are relatively complex functions of D and Δ.[9,19,20] Simple situations are attained only in the weak-coupling limit, defined by $D \ll \Delta$, and in the very-strong coupling limit, $D \gg \Delta$, since in these limits the noncommutation problem is effectively removed. The case of $D \sim \Delta$ will be referred to as the intermediate coupling regime (it has also been termed the strong-coupling regime[21]). In solution NMR at high fields, the J coupling is usually in the weak limit (AX system), while in solids the limit of very strong dipolar coupling (A_2 system) is encountered quite often: For protons in solids, chemical-shift differences are small and dipolar couplings large, while in ^{13}C NMR, the chemical-shift difference sometimes vanishes for symmetry reasons. This is the case for the polyethylene sample used in this study. The expressions for density-operator time evolutions, spectra, etc., under the dipolar coupling in the two simple limits are usually very similar. In both limits, the spectra for a single segment with the $^{13}C-^{13}C$ bond making an angle θ with the B_0 field exhibit doublets with splittings of

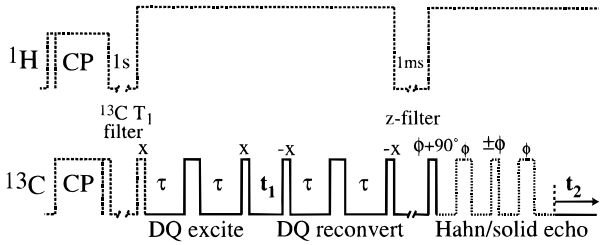

Figure 2. Pulse sequence for solid-state 2D NMR with double-quantum evolution (double-quantum spectroscopy, DOQSY), which yields a spectrum reflecting the sum of the chemical shift in the first dimension. It is basically the refocused INADEQUATE sequence[21–27] (full line), modified for the application to solid polymers (dashed lines). The signal is generated by cross-polarization, the amorphous-phase signal is removed by a T_1 filter, and the dead-time problem is avoided by a solid echo with Hahn-echo sandwich[28] before detection.

$$2\omega_D = 2q \times 7.6 \text{ kHz Å}^3/r^3(3\cos^2\theta - 1)/2 \qquad (1)$$

In the very-strong coupling limit, there is a single doublet with a prefactor $q = {}^3/_2$ in the splitting of eq 1, centered at the common chemical shift position (this differs from the strong-coupling limit of the J-coupling, where no splitting is observed, due to a simpler form of the Hamiltonian). In the weak-coupling limit, two doublets arise, each centered at the chemical-shift positions of one of the coupled sites, with splittings which are two-thirds of that in the strong limit ($q = 1$ in eq 1).

In the following, we briefly review the principle of the double-quantum pulse sequence shown in Figure 2, which is similar to the refocused INADEQUATE sequence used in solution NMR.[21–27] We consider a pair of ^{13}C spins, S and L, in two bonded sites with chemical shifts ω_a (L spin) and ω_b (S spin). The analysis is simple in the cases of the weak and the very-strong coupling limits, where the chemical shift and the (effective) dipolar coupling in the overall Hamiltonian H commute and can be treated independently. The evolution of y magnetization under the central part of the pulse sequence in Figure 2 can be sketched as follows (retaining only the relevant terms, which are selected by phase cycling):

$$\begin{aligned} S_y + L_y &\xrightarrow{H\tau}\xrightarrow{180°}\xrightarrow{H\tau} (S_xL_z + S_zL_x)g(2\tau) \xrightarrow{90°x} \\ &(S_xL_y + S_yL_x)g(2\tau) \xrightarrow{Ht_1} \\ &(S_xL_y + S_yL_x)g(2\tau)\cos(\omega_a + \omega_b)t_1 \xrightarrow{90°(-x)} \\ &(S_xL_z + S_zL_x)g(2\tau)\cos(\omega_a + \omega_b)t_1 \xrightarrow{H\tau}\xrightarrow{180°}\xrightarrow{H\tau} \\ &(S_y + L_y)g^2(2\tau)\cos(\omega_a + \omega_b)t_1 \xrightarrow{Ht_2} \end{aligned} \qquad (2)$$

Here, $g(2\tau) = q\{-2\sin(\omega_D 2\tau)\}$ in both limits, with $q = 1$ in the weak and $q = {}^3/_2$ in the very-strong coupling limit, and ω_D given by eq 1. Nakai and McDowell[27] have

performed a full product-operator analysis for the general case of arbitrary coupling strength, which showed that the spin terms and the $\cos(\omega_a + \omega_b)t_1$ modulation are always as given in eq 2. The only modification is that $g(\tau)$ becomes a more complicated function. In the calculations of the double-quantum spectra shown below, we always incorporated the exact τ dependence as given in ref 27.

To obtain selectively the terms given in eq 2, phase cycling must be applied. Most importantly, the signal arising from z magnetization in the t_1 period must be suppressed. This can be achieved by shifting the pulse phases and exploiting the following differences in signs:

$$\begin{aligned}(S_xL_y + S_yL_x) &\xrightarrow{90°x} -(S_xL_z + S_zL_x) \xrightarrow{H_{dip}} + S_y,\\ S_z &\xrightarrow{90°x} + S_y\\ (S_xL_y + S_yL_x) &\xrightarrow{90°y} (S_zL_y + S_yL_z) \xrightarrow{H_{dip}} + S_x\\ S_z &\xrightarrow{90°y} - S_x\end{aligned} \qquad (3)$$

At the end of the reconversion period, we use a z filter to obtain purely absorptive spectra. To avoid baseline distortions resulting from pulse ring-down and receiver deadtime, before the detection we refocus the magnetization by a combination of two Hahn echoes with a solid echo, as will be discussed in detail elsewhere.[28]

The double-quantum pulse sequence in Figure 2 is similar to the refocused INADEQUATE sequence used for obtaining connectivity information in solution NMR, and in its details it greatly benefits from a decade of improvements[21,25−27] made to the original INADEQUATE idea.[22−24] However, the application to solids introduced here puts the sequence into a new context, since the spectra in static solids and in solution have a completely different appearance and interpretation. In solution NMR and in most of the related double-quantum solid-state NMR experiments to date,[16,29−34] INADEQUATE is used to trace out connectivities of many sites by inspection of peak positions. In contrast, in our experiments, the relative orientation of two tensors is determined from two-dimensional ridge patterns, as will be discussed in the following. As far as terminology is concerned, INADEQUATE (incredible natural-abundance double quantum experiment) would be an inadequate description, since our experiment requires specific isotopic labeling. We suggest the term DOQSY (double-quantum spectroscopy) in analogy to COSY, NOESY, TOCSY, etc.[21]

Relative Segmental Orientations from Double-Quantum NMR. The t_1 dependence in eq 2, which is given by $\cos(\omega_a + \omega_b)t_1$, contains information on the relative orientation of the chemical-shift principal-axes systems of the coupled sites a and b. The dependence on the torsion angle ψ becomes apparent by calculating the frequencies ω_a and ω_b (in ppm of the Larmor frequency) with the chemical-shift tensors σ_a and σ_b expressed in a common frame. For example, this reference system can be chosen to coincide with the principal-axes system (PAS) of σ_a:

$$\begin{aligned}\omega_a &= \vec{b}_0^{\,T}(\theta,\phi)\, \sigma_a \vec{b}_0(\theta,\phi)\\ \omega_b &= \vec{b}_0^{\,T}(\theta,\phi)\, \mathbf{R}_{b\to a}(\psi)\, \sigma_b \mathbf{R}_{b\to a}^{T}(\psi)\, \vec{b}_0(\theta,\phi)\end{aligned} \qquad (4)$$

with the matrix of rotation from the PAS of σ_a to the PAS of σ_b:

$$\begin{aligned}\mathbf{R}_{b\to a}(\psi) &= \tilde{\mathbf{R}}^{T}(\alpha_a,\beta_a,0)\, \tilde{\mathbf{R}}(\alpha_b,\beta_b,-\psi)\\ &= \tilde{\mathbf{R}}(0,-\beta_a,-\alpha_a)\, \tilde{\mathbf{R}}(\alpha_b,\beta_b,-\psi)\end{aligned} \qquad (5)$$

Here, $\vec{b}_0(\theta,\phi)$ is the unit vector along the B_0-field direction, characterized by its polar coordinates (θ,ϕ) in the PAS of σ_a. $\tilde{R}(\alpha_b,\beta_b,-\psi)$ is the active-rotation matrix[6] for Euler angles $(\alpha_b,\beta_b,-\psi)$ that rotate the z axis of the principal-axes system of the chemical-shift tensor of site b onto the C−C internuclear vector and by $(-\psi)$ around this vector. In other words, (β_a,α_a) are the polar coordinates of the C−C internuclear vector in the PAS of σ_a.

Note that for a powder spectrum reflecting the individual frequency ω_a, the integration over θ and ϕ makes the spectrum independent of the absolute orientation of individual segments, i.e., of angles such as α_a, β_a, and ψ. The powder pattern depends only on the principal values of σ_a (or, equivalently, on the parameters $\delta_a = (\sigma_{a,33} - \sigma_{a,iso})$ and $\eta_a = |\sigma_{a,22} - \sigma_{a,11}|/\delta_a$ derived from them). The same applies for the powder pattern reflecting ω_b, since we can consider the isotropic averaging in the principal-axes system of σ_b. In contrast to this, the powder spectrum of the sum of the frequencies ω_a and ω_b depends on the principal values of the sum tensor:

$$\sigma_a + \tilde{\mathbf{R}}^{T}(\alpha_a,\beta_a,0)\, \tilde{\mathbf{R}}(\alpha_b,\beta_b,-\psi)\, \sigma_b \tilde{\mathbf{R}}^{T}(\alpha_b,\beta_b,-\psi)\, \tilde{\mathbf{R}}(\alpha_a,\beta_a,0) \qquad (6)$$

and therefore retains information on the relative orientation of the two principal-axes systems. The determination of the principal values of the sum tensor is identical with the calculation of the motionally averaged line shape for fast jumps between the sites a and b. This may be helpful if the ω_2 dimension in the DOQSY spectrum is complicated by dipolar couplings in the intermediate-coupling regime. In general, however, much more reliable torsion-angle values can be obtained by the correlation of the sum frequencies with other interactions in a two-dimensional NMR experiment, as discussed in the following.

From other two-dimensional correlation experiments, it is well-known that 2D powder spectra exhibit ridge patterns, often tracing out ellipses and triangles, which are characteristic of the relative orientation of the NMR interaction tensors that are correlated along the two dimensions of the spectrum.[6,35,36] In our experiments, we correlate the sum chemical shift $(\omega_a + \omega_b)$ with the individual chemical shifts $\omega_{a,b}$ and the dipolar coupling frequency ω_D (defined by eq 1, with $q = {}^3/_2$). In the very-strong and weak coupling limits, each segment yields four signals, at $(\omega_a + \omega_b, \omega_a \pm \omega_D)$ and $(\omega_a + \omega_b, \omega_b \pm \omega_D)$. This leads to four sets of ridge patterns. In the very-strong coupling limit, pairs of these patterns can become degenerate for symmetry reasons. This is the case in the polyethylene spectra shown below. In the weak-coupling limit, the pairs of patterns for $(\omega_a + \omega_b, \omega_a \pm \omega_D)$ and for $(\omega_a + \omega_b, \omega_b \pm \omega_D)$ are well separated in the ω_2 dimension. A calculated spectrum for this case is shown in Figure 3. The ridge patterns for the two sites can be seen to have similar shapes. Writing $\Omega = \omega_a + \omega_b$, we have patterns of

$$(\omega_1, \omega_2) = (\omega_a + \omega_b, \omega_a \pm \omega_D) = (\Omega, \omega_a \pm \omega_D) \qquad (7a)$$

$$(\omega_1, \omega_2) = (\omega_a + \omega_b, \omega_b \pm \omega_D) = (\Omega, \Omega - \{\omega_a \pm \omega_D\}) \qquad (7b)$$

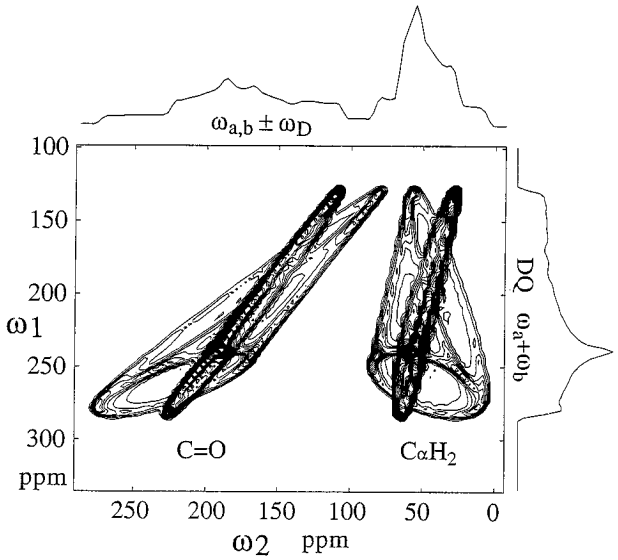

Figure 3. Calculated DOQSY solid-state NMR spectrum in the weak coupling limit (the calculation was nevertheless performed for the general case,[9,27] without weak-coupling approximation). The parameters were those of a glycine residue in a peptide with labeled C=O and $C_\alpha H_2$ sites, as given in the caption of Figure 5 below, with a torsion angle of ψ = 0° (i.e., 180° relative to the trans conformation).

Comparison of the expressions on the right-hand sides shows that the pattern of eq 7b is that of eq 7a inverted in the ω_2 dimension and, by the added Ω, sheared by 45° along ω_2. This corresponds to the observed patterns in Figure 3. In the intermediate-coupling regime, the spectrum along the ω_2 dimension becomes more complex in terms of the positions and intensities of the four peaks.[9] Nevertheless, the peaks are still located at a single $\omega_1 = \omega_a + \omega_b$.

The range of torsion angles that yield different 2D spectral patterns can cover the full range of 360°. This was proven by the variations of a set of simulated 2D spectra for a given pair of sites, with the torsion angle incremented in small (20°) steps over 360° (not shown). By contrast, the reorientation-angle distribution accessible in 2D exchange NMR patterns from uniaxial interactions (e.g., the quadrupolar interaction for ^{2}H in a CH_n moiety) has a range of only 90°.[6] One reason for this difference is the fact that the torsion or rotation angle and the reorientation angle, though related, are usually not identical.[6] Only when one of the tensors is uniaxial and the unique principal axis perpendicular to the internuclear bond does the torsion angle coincide with the reorientation angle of the unique axis. In this specific case, the unique range of the spectral patterns covers only 90°. For pairs of chemically identical sites (as in polyethylene) and for systems where at least one principal axis for each site is perpendicular to the internuclear vector (which is always the case for a uniaxial interaction), the torsion-angle range of unique spectral 2D patterns is reduced from 360° to 180°. This applies for the polyethylene and peptide segments considered in this paper. In both of these cases, the symmetries of the chemical-shift tensor orientations are such that the spectra for $\pm\psi$ are identical, over the range ψ = 0−180°.

Comparison with Other NMR Experiments for Torsion-Angle Measurement. The usefulness of the DOQSY experiment for torsion-angle measurements derives from the fact that the signal in the double-quantum dimension reflects the sum of the chemical shifts. By contrast, the correlation of the *individual* chemical shift with the dipolar coupling often does not provide information on the torsion angle. The resulting spectral patterns in the weak and very-strong coupling limits depend solely on the orientation of the $^{13}C-^{13}C$ bond, the unique axis of the dipolar interaction, in the chemical-shift PAS. Only in the intermediate coupling regime does the spectrum resulting from dipolar coupling and individual chemical shifts acting together become dependent on the torsion angle, as was recently pointed out by Nakai and McDowell.[9] However, due to the multiple splittings of the signal from each crystallite, the spectra are quite complex and the torsion angles are rather difficult to extract. Often, only minor features of the spectra depend on the conformation.[9]

At this point, it is also interesting to compare our technique with a recent application of rotational resonance[7] that focused on the relative chemical-shift tensor orientation (rather than determining dipolar couplings and internuclear distances as is more common in rotational resonance[11,12]). The technique exploits that rotational resonance of high order reflects the chemical-shift difference tensor of two ^{13}C-labeled sites. Compared to the double-quantum experiment, the rotational-resonance technique provides a better signal-to-noise ratio, since the detected signal intensity under magic-angle spinning is compressed into few center- and sidebands. This makes larger molecules accessible.

However, the rotational−resonance technique is not applicable to sites with small or vanishing differences in their isotropic chemical shifts. For example, the MAS experiment would not be applicable to the polyethylene sample used in this study, since the labeled sites have identical isotropic chemical shifts (restricting rotational resonance to a single order n = 0). For the backbones of many synthetic polymers, the differences in the isotropic chemical shifts are small (<20 ppm), so that the rotational resonance with $n \geq 4$ becomes difficult to perform, requiring very small rotation rates (<5 ppm) which are comparable to the widths of the sidebands.

In addition, the rotational−resonance experiment does not provide sufficient resolution for studying polypeptides, according to ref 7. This is a consequence of the relatively low angular resolution, which in turn is due to the one-dimensional nature of the experiment. By contrast, the double-quantum 2D patterns for glycine residues in peptides shown below vary significantly with the torsion angle. Also, from the rather featureless intensity decay measured in rotational resonance, information on the torsion-angle distribution is hardly accessible. By contrast, in the DOQSY experiment a broad or multimodal distribution of torsion angles would be indicated by increased broadening or complexity of the 2D pattern and by the deviation of the projection on the double-quantum axis from a single powder pattern.

Results and Discussion

Figure 4a shows a double-quantum 2D spectrum of the crystalline regions of $^{13}C-^{13}C$ labeled PE, obtained with the pulse sequence of Figure 2. As discussed above, the spectrum correlates the sum of the chemical shifts of the two sites, along ω_1, with the sum of the individual chemical shift and the dipolar coupling, along ω_2. The spectrum exhibits triangular and elliptical ridge patterns, which are sensitive to the torsion angle between the two sites (and to their chemical-shift tensor orientations). Figure 4b displays the simulation for a

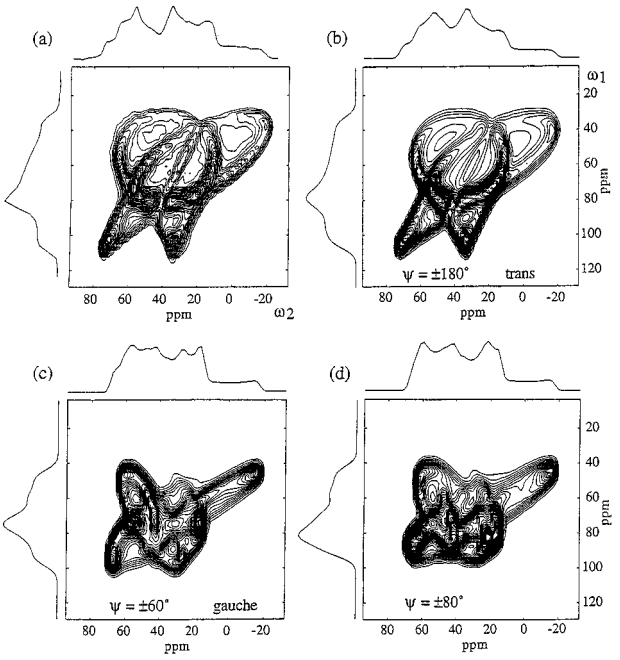

Figure 4. (a) Experimental DOQSY NMR spectrum of 4% ^{13}C spin-pair labeled polyethylene correlating the sum chemical shift with the dipolar coupling and individual chemical shifts. Due to the T_1 filter in the pulse sequence, signal from the crystalline regions is observed selectively. (b) Corresponding simulation, with an effective C−C bond length of 1.5 (6 ± 2) Å, a bond angle of 113°, chemical-shift principal values of 50.3, 35.8, and 12.5 ppm, and polar coordinates ($\alpha = 270°$, $\beta = 33.5°$) of the C−C bond in the conventional chemical-shift PAS of the crystalline regions of polyethylene.[38] (c) Simulation for a gauche conformation, $\psi = \pm 60°$. (d) Simulation for $\psi = \pm 80°$. Note in particular the change, compared to (c), of the projection on the ω_1 (vertical) axis. The simulations use exact equations derived by Nakai and MacDowell for the most general case of the refocused INADEQUATE pulse sequence[27] and the dipolar/chemical-shift spectrum.[9] The spectra in (c) and (d) are complicated in the ω_2 dimension because the system is mostly in the intermediate-coupling regime.

trans conformation, using the known ^{13}C chemical-shift tensor orientation in polyethylene, shown in Figure 1a, which conforms with the segmental symmetries (principal axes perpendicular to the symmetry planes).[37,38] For a gauche conformation, a drastically different line shape would be found, as shown in Figure 4c for $\psi = \pm 60°$. Not only are the relative orientations of the coupled chemical-shift tensors different, but the system is also in the intermediate-coupling regime: The chemical shifts of the two sites are different since their chemical shift tensors are not parallel for a gauche conformation, and these frequency differences are comparable to the strength of the dipolar coupling. This complicates the spectrum in the ω_2 dimension and thus also the 2D spectrum. Still, the spectrum is free of dipolar splittings in the double-quantum ω_1 dimension, which makes the patterns amenable to a relatively simple analysis. The pattern in the spectrum of Figure 4d, which was simulated for a gauche torsion angle differing by 20° from that in Figure 4c, is significantly different, which indicates that an angular resolution of down to ±10° can be achieved.

The example of Figure 4 shows that the determination of the torsion angle is based on the comparison of the experimental 2D powder pattern with its simulated counterparts. The search for the best fit can be performed either visually or by a least-squares analysis. In this context, it is important to note that the torsion angle is the only relevant unknown parameter in the fit. This makes the analysis much simpler than the analysis of the geometry of molecular motions from 2D spectra, where arbitrary rotations, characterized by three Euler angles, must be considered.[6] Other parameters that affect the DOQSY 2D patterns, such as the chemical-shift tensor orientation and the dipolar coupling strength, can be determined in independent auxiliary NMR experiments on the same sample, strongly reducing the effects of the intrinsic dependence of the chemical-shift tensor on the conformation of neighboring segments.

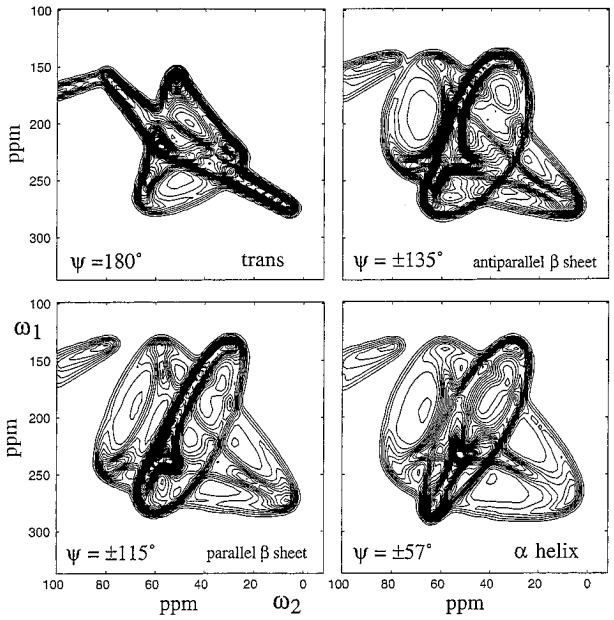

Figure 5. Simulated DOQSY NMR spectra for a glycine residue in a peptide with labeled C=O and C_α sites. Principal values of ($\sigma_{11} = 244$ ppm, $\sigma_{22} = 177$ ppm, $\sigma_{33} = 87.4$ ppm) for the C=O and ($\sigma_{33} = 66$ ppm, $\sigma_{22} = 46$ ppm, $\sigma_{33} = 27$ ppm) for the C_α site were used. The orientation of the C=O chemical-shift tensor was taken from the literature, with the C−C bond oriented at polar coordinates of $\alpha = 17°$ and $\beta = 90°$ in the PAS.[39] For simplicity, the tensor orientation for the $C_\alpha H_2$ group was assumed to be that of an ideal methylene group, as for polyethylene above, which seems to be a reasonable approximation.[37] In a real system, these tensor orientations would be measured by correlating the chemical shift with dipolar couplings.[35,36] For simplicity, $^{14}N-^{13}C$ couplings were not considered in the simulations shown here. The calculations of the effects of the $^{13}C-^{13}C$ couplings were performed without approximations, but the spectra show that the system is in the weak-coupling limit, as expected with the large chemical-shift difference. Spectra for eight durations $2\tau = 200$, 400, ..., 1600 μs of double-quantum excitation were co-added. Shown here are contour plots (3−95% of maximum intensity) for the spectral region of the C_α signal (100 to −10 ppm) in ω_2, for various torsion angles ψ. The full projection on the ω_2 axis and the similar shape of the 2D pattern of the ^{13}C=O site are demonstrated in Figure 3 above. From upper left to lower right, the torsion angle ψ has values of 180° (trans conformation), ±135° (antiparallel β sheet), ±115° (parallel β sheet), and ±57° (α helix), as indicated below the plots. Note the variations of both the outlines of the patterns and of the intensity distributions within them.

The double-quantum experiment presented here appears promising for the elucidation of peptide conformations. The torsion angle ψ in a doubly ^{13}C labeled amino acid residue can be determined by characterizing the relative orientation of the C=O and the C_α units. Figure 5 displays DOQSY 2D spectra simulated with the parameters typical of a glycine residue,[37,39] as indicated in Figure 1b. The spectral intensity patterns

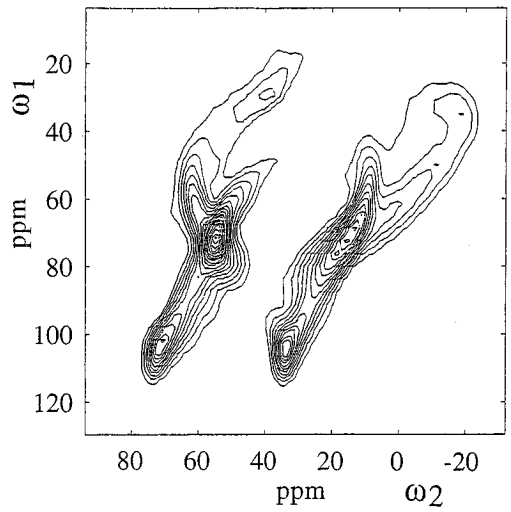

Figure 6. Signal-to-noise demonstration for the DOQSY experiment: A measuring time of 1 h (1024 scans total) yields a 2D spectrum of the 4% $^{13}C-^{13}C$ labeled polyethylene where the lowest contour level, at 10% of the maximum, is still above the noise level. The pulse sequence was the same as for the spectrum in Figure 4a, but due to the measuring-time constraint and the minimum phase cycle of 32 steps, only one duration, $2\tau = 120$ μs, was used for the double-quantum generation. Therefore, the line shape is altered compared to Figure 4a, consistent with corresponding simulations (not shown).

vary considerably with the torsion angle and should allow for a determination of ψ with a precision of down to $\pm 10°$. Due to the large difference in the isotropic chemical shifts of the two sites (>9 kHz at 75 Hz/ppm), the system is mostly in the weak-coupling limit, yielding relatively clear and simple 2D patterns. Unfortunately, some complications will arise in practice from the dipolar couplings to the adjacent ^{14}N nuclei in the peptide backbone. The resulting line broadening of approximately 800 Hz is relatively large, but preliminary experiments and simulations show that the overall features of the 2D spectral patterns are still observable.

The synthesis of doubly ^{13}C-labeled samples for the double-quantum experiment will be relatively convenient because only a single doubly ^{13}C-labeled amino acid residue needs to be introduced into the peptide, which can often be achieved by biosynthetic techniques. In contrast to this, two labeled residues are required for other NMR structure-determination techniques, such as rotational resonance[11,12] or REDOR/TEDOR,[13−15] which obtain torsion angles from long-range dipolar couplings.

The sensitivity problem of NMR will be the main limitation to the size or complexity of polypeptides that can be investigated by the DOQSY technique. We estimate that with 200 mg of a polypeptide in which 1 of 20 residues is doubly ^{13}C labeled (i.e., with 3% of the backbone atoms and ~1% of all carbon atoms labeled), a DOQSY 2D spectrum yielding the torsion angle can be acquired in 48 h. To corroborate this point, Figure 6 shows a DOQSY 2D spectrum of the 4%-labeled PE sample (~400 mg) acquired in 1 h (1024 scans in total). The noise level is below the lowest contour line, which is at 10% of the spectral intensity maximum. In a 48-h measurement with a recycle delay of 1.5 s (115 000 scans), the signal-to-noise ratio will be increased by a factor of 10, compensating for various factors that diminish the signal from a polypeptide sample (and giving ample time for averaging over several τ values, for excitation of the full 2D pattern). Signal reduction by isotopic dilution, which is required for accurate distance determinations by rotational resonance[11,12] or REDOR/TEDOR,[13−15] can be avoided with our technique, since the directly bonded coupling dominates over all intermolecular ones.

Summary and Outlook

We have presented a double-quantum solid-state NMR technique for correlating the chemical-shift tensors in pairs of bonded ^{13}C-labeled sites. It provides relatively simple two-dimensional spectral patterns by eliminating the dipolar coupling in one spectral dimension, by suppressing the natural-abundance background signals, and by inherently removing the intense diagonal ridge that dominates related 2D exchange spectra. From the two-dimensional pattern, the torsion angle which characterizes the relative orientation of the ^{13}C-labeled sites can be determined with relatively high precision. This was demonstrated by an experimental 2D spectrum of the crystalline regions of unoriented $^{13}C-^{13}C$ labeled polyethylene, which was compared with simulated spectra for various conformations. The technique will be applicable to many suitably ^{13}C-labeled synthetic and biological polymers. Since the double ^{13}C label can often be introduced via a single monomer unit, the isotopic labeling will be relatively convenient. We estimate that the signal-to-noise ratio will be sufficient for characterizing one doubly ^{13}C-labeled amino acid residue in a polypeptide repeat unit with a molar mass of up to 2000 g/mol.

Acknowledgment. The author would like to thank Dr. C. Boeffel and Prof. H. W. Spiess for making the doubly ^{13}C-labeled polyethylene sample available and Dr. L. C. Dickinson for excellent hardware support and for checking the manuscript. M. Hong, Dr. D. J. Schaefer, and Prof. L. K. Thompson also provided helpful comments on the text. Financial support from the National Science Foundation is gratefully acknowledged.

References and Notes

(1) Henrichs, P. M.; Linder, M. *J. Magn. Reson.* **1984**, *58*, 458.
(2) Edzes, H. T.; Bernards, J. P. C. *J. Am. Chem. Soc.* **1984**, *106*, 1515.
(3) Robyr, P.; Meier, B. H.; Ernst, R. R. *Chem. Phys. Lett.* **1991**, *187*, 471.
(4) Dabbagh, G.; Weliky, D. P.; Tycko, R. *Macromolecules* **1994**, *27*, 6183.
(5) Robyr, P.; Tomaselli, M.; Straka, J.; Grob-Pisano, C.; Suter, U. W.; Meier, B. H.; Ernst, R. R. *Mol. Phys.* **1995**, *84*, 995.
(6) Schmidt-Rohr, K.; Spiess, H. W. *Multidimensional Solid-State NMR and Polymers*; Academic Press: London, 1994.
(7) Tomita, Y.; O'Connor, E. J.; McDermott, A. *J. Am. Chem. Soc.* **1994**, *116*, 8766.
(8) Weliky, D. P.; Dabbagh, G.; Tycko, R. *J. Magn. Reson. A* **1993**, *104*, 10.
(9) Nakai, T.; McDowell, C. A. *Chem. Phys. Lett.* **1994**, *217*, 234; *J. Am. Chem. Soc.* **1994**, *116*, 6373.
(10) Tomaselli, M.; Meier, B. H.; Robyr, P.; Suter, U. W.; Ernst, R. R.: Poster Abstract 180, Experimental NMR Conference, Boston, 1995.
(11) Raleigh, D. P.; Creuzet, F.; Das Gupta, S. K.; Levitt, M. H.; Griffin, R. G. *J. Am. Chem. Soc.* **1989**, *111*, 4502.
(12) Bennett, A.; Griffin, R. G.; Vega, S. *NMR Basic Principles Progr.* **1994**, *33*, 3.
(13) Gullion, T.; Schaefer, J. *Adv. Magn. Reson.* **1989**, *13*, 57.
(14) Pan, Y.; Gullion, T.; Schaefer, J. *J. Magn. Reson.* **1990**, *90*, 330.
(15) Hing, A.; Vega, S.; Schaefer, J. *J. Magn. Reson.* **1992**, *96*, 205.
(16) Gottwald, J.; Demco, D. E.; Graf, R.; Spiess, H. W., submitted to *Chem. Phys. Lett.*

(17) Jeener, J.; Meier, B. H.; Bachmann, P.; Ernst, R. R. *J. Chem. Phys.* **1979**, *71*, 4546.
(18) Pines, A.; Gibby, M. G.; Waugh, J. S. *J. Chem. Phys.* **1973**, *59*, 569.
(19) Abragam, A. *The Principles of Nuclear Magnetism*; Oxford University Press: London, 1961; pp 484−487.
(20) Zilm, K.; Grant, D. *J. Am. Chem. Soc.* **1981**, *103*, 2913.
(21) Ernst, R. R.; Bodenhausen, G.; Wokaun, A. *Nuclear Magnetic Resonance in One and Two Dimensions*; Oxford University Press: Oxford, 1987.
(22) Bax, A.; Freeman, R.; Kempsell, S. P. *J. Am. Chem. Soc.* **1980**, *102*, 4849.
(23) Bax, A.; Freeman, R. *J. Magn. Reson.* **1980**, *41*, 507.
(24) Bax, A.; Freeman, R.; Frankiell, T.; Levitt, M. H. *J. Magn. Reson.* **1981**, *43*, 478.
(25) Mareci, T. H.; Freeman, R. *J. Magn. Reson.* **1982**, *48*, 158.
(26) Sørensen, O. W.; Levitt, M. H.; Ernst, R. R. *J. Magn. Reson.* **1983**, *55*, 104.
(27) Nakai, T.; McDowell, C. A. *Mol. Phys.* **1993**, *79*, 965.
(28) Schmidt-Rohr, K., to be published.
(29) Vega, S.; Pines, A. *J. Chem. Phys.* **1977**, *66*, 5624.
(30) Menger, E. M.; Vega, S.; Griffin, R. G. *J. Magn. Reson.* **1984**, *56*, 338.
(31) Menger, E. M.; Vega, S.; Griffin, R. G. *J. Am. Chem. Soc.* **1986**, *108*, 2215.
(32) Meier, B. H.; Earl, W. L. *J. Chem. Phys.* **1985**, *85*, 4905.
(33) Tycko, R.; Dabbagh, G. *J. Am. Chem. Soc.* **1991**, *113*, 9444.
(34) Levitt, M. *J. Chem. Phys.* **1994**, *101*, 1805.
(35) Linder, M.; Höhener, A.; Ernst, R. R. *J. Chem. Phys.* **1980**, *73*, 4959.
(36) Terao, T.; Miura, H.; Saika, A. *J. Chem. Phys.* **1986**, *85*, 3816.
(37) Veeman, W. S. *Prog. NMR Spectrosc.* **1984**, *16*, 193.
(38) VanderHart, D. L. *J. Chem. Phys.* **1976**, *64*, 830.
(39) Stark, R. E.; Jelinski, L. W.; Ruben, D. J.; Torchia, D. A.; Griffin, R. G. *J. Magn. Reson.* **1983**, *55*, 266.

MA9517106